Spatial clustering and repeating of seismic events observed along the 1976 Tangshan fault, north China

Le Li,[1,2,3] Qi-Fu Chen,[2] Xin Cheng,[3] and Fenglin Niu[2,3]

Received 8 August 2007; revised 10 November 2007; accepted 12 November 2007; published 13 December 2007.

[1] Spatial and temporal features of the seismicity occurring along the Tangshan fault in 2001–2006 were investigated with data recorded by the Beijing metropolitan digital Seismic Network. The relocated seismicity with the double difference method clearly exhibits a dextral bend in the middle of the fault. More than 85% of the earthquakes were found in the two clusters forming the northern segment where relatively small coseismic slips were observed during the 1976 M7.8 earthquake. The *b* values calculated from the seismicity occurring in the northern and southern segment are 1.03 ± 0.02 and 0.85 ± 0.03, respectively. The distinct seismicity and *b* values are probably the collective effect of the fault geometry and the regional stress field that has an ENE-WSW oriented compression. Using cross-correlation and fine relocation analyses, we also identified a total of 21 doublets and 25 multiplets that make up >50% of the total seismicity. Most of the sequences are aperiodic with recurrence intervals varying from a few minutes to hundreds of days. Based on a quasi-periodic sequence, we obtained a fault slip rate of $\leq$2.6 mm/yr at $\sim$15 km, which is consistent with surface GPS measurements. **Citation:** Li, L., Q.-F. Chen, X. Cheng, and F. Niu (2007), Spatial clustering and repeating of seismic events observed along the 1976 Tangshan fault, north China, *Geophys. Res. Lett.*, *34*, L23309, doi:10.1029/2007GL031594.

1. Introduction

[2] The surface of North China is marked by its unusually active tectonic movement and high intraplate seismicity, especially strong and devastated earthquakes. The magnitude 7.8 earthquake that struck the city of Tangshan, $\sim$160 km east of Beijing, on July 28, 1976 is one of the most destructive events in terms of the loss of life. The earthquake occurred on the northern margin of the North China sedimentary basin near the boundary between the basin and Yanshan uplift. The main shock fault is a NE trending strike-slip faulting system [*Shedlock et al.*, 1987; *Nabelek et al.*, 1987] with a dextral bend in the middle that divides the fault into the southern and northern segments (Figure 1). High seismicity has been maintained since the earthquake along the main fault. To better monitor the seismic activity in the capital area, the Chinese Earthquake Administration (CEA) started to deploy the Beijing metropolitan digital Seismic Network (BSN) in the late 90s. Currently the network consists of 107 broadband, borehole and surface short-period stations that covers an area of $\sim$180,000 km^2 including Beijing, Tianjin and Tangshan metropolitan cities (Figure 1). Since 2001, a large amount of data including waveform data has been collected. The data provide a new opportunity for investigating the spatial and temporal features of the seismicity along the Tangshan fault.

[3] Fine relocation of seismicity along a fault not only provides a direct 3D view of the fault structure [e.g., *Waldhauser and Ellsworth*, 2002], but also shed lights on earthquake physics [*Rubin et al.*, 1999]. *Gutenberg and Richter* [1944] found that the earthquake size distribution in California follows a power law. The slope of this power law, the '*b*-value', is commonly used to describe the relative occurrence of large and small events. Laboratory studies [e.g., *Scholz*, 1968] found that *b* values are inversely dependent on differential stress. Recent studies [e.g., *Schorlemmer and Wiemer*, 2005] confirmed this dependence from field data.

[4] Repeating earthquakes are a series of earthquakes regularly occurring on a patch of a fault plane. These earthquakes usually have approximately the same magnitude with roughly the same repeating interval. They are commonly interpreted as repeated ruptures of a single asperity surrounded by a stably sliding area. Repeating earthquakes have been observed in the creeping zones of major faults along plate boundaries [*Vidale et al.*, 1994; *Igarashi et al.*, 2003]. Using teleseismic waveform data, *Schaff and Richards* [2004] found that $\sim$10% of the seismic events in China were repeating earthquakes. *Nadeau and Johnson* [1998] used the scalar moment and recurrence interval of repeating earthquakes to infer fault slip rate at depth.

[5] In this study, we analyzed the catalog, local and regional waveform data of more than 1000 earthquakes occurring between 2001 and 2006 in the aftershock zone of the 1976 Tangshan earthquake to study the spatial distribution, similarity and repeatability of these events. We first relocated earthquakes using the double-difference (DD) algorithm [*Waldhauser and Ellsworth*, 2000] and then applied waveform cross-correlation methods to identify similar and repeating earthquakes.

2. Data and Analysis

[6] In this study we used the data collected by the BSN between October of 2001 and December of 2006. There are a total of 1020 events ($0.5 \leq M \leq 4.1$) that occurred along the main Tangshan fault (rectangle in Figure 1) in the period. To avoid waveform complication from the head

[1]Institute of Geophysics, China Earthquake Administration, Beijing, China.
[2]Institute of Earthquake Science, China Earthquake Administration, Beijing, China.
[3]Department of Earth Science, Rice University, Houston, Texas, USA.

0094-8276/07/2007GL031594$05.00

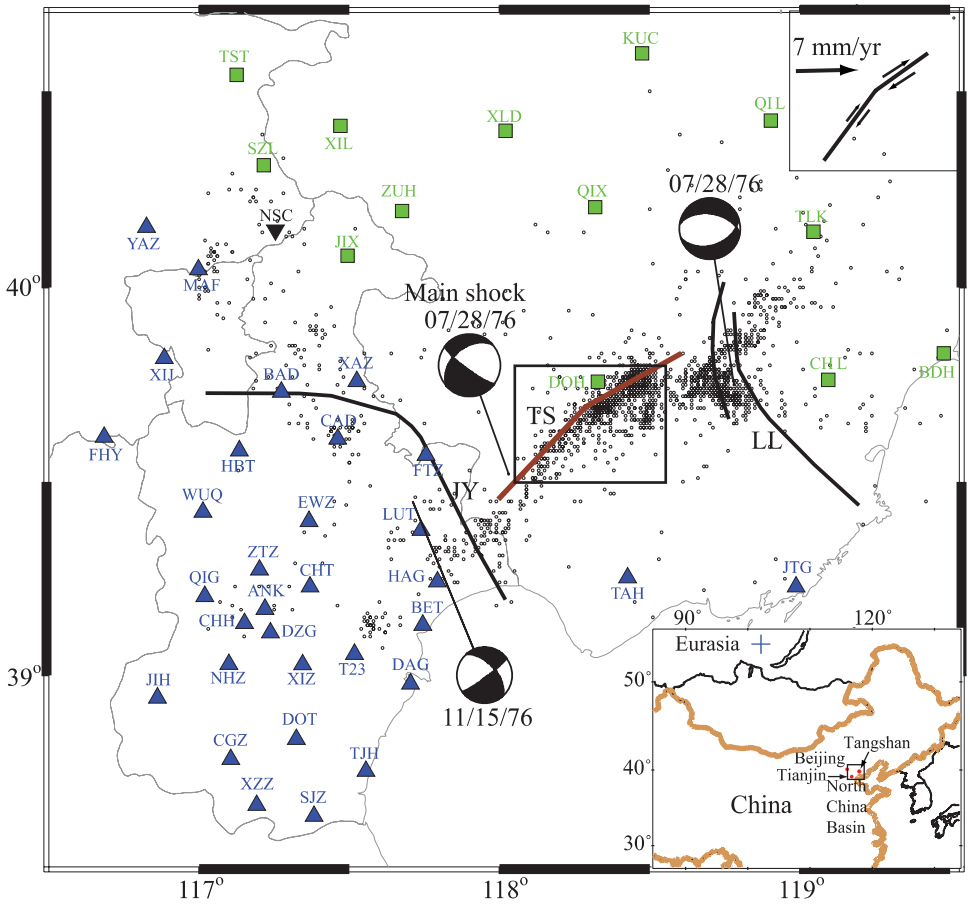

Figure 1. Geographic map showing the 1976 Tangshan earthquake series, major faults, and BSN stations. Fault locations are from *Shedlock et al.* [1987]. TS, Tangshan main Fault; JY, Jiyunhe Fault; LL, Luanxian-Leting Fault. Squares, triangles, and reverse triangle indicate broadband, borehole, and surface short-period stations, respectively. Circles indicate earthquakes ($0.3 < M_L < 5.0$) occurring between 10/2001 and 12/2006. Only earthquakes inside the box were relocated. Upper inset illustrates the bend of the Tangshan fault with the arrow indicating the eastward motion of the North China basin relative to the stable Eurasia that is indicated by the cross in the lower inset.

wave Pn, we selected a total of 46 stations that are located within 150 km from the main fault (Figure 1). We have 9184 picks of P-wave arrival times from the BSN bulletins. Among the 1020 events, there are 619 events whose waveform data are available to us.

[7] Catalog locations were routinely determined from picks of P- and S-wave arrival times. Typical precision of location error is in the order of a few kilometers to a couple tens of kilometers. To better resolve the 3D seismicity, we used the DD method to relocate the events. The DD method minimizes residuals between the observed differential times measured from pairs of earthquakes at each station and those calculated times. Instead of locating each event individually the DD method is designed to derive a set of locations that best fit the relative travel times among the entire seismicity. Especially when accurate differential travel-time data are available from waveform cross correlation (cc), the DD method has been proved to be able to collapse diffuse catalog locations into sharp images of seismicity [e.g., *Waldhauser and Ellsworth*, 2002].

[8] In addition to the bulletin picks, we also used a cc based method to measure accurate differential times between pairs of events. To do this, a 1–10 Hz bandpass filter was first applied to the data. As the sampling rate of the BSN stations is 50 Hz, an interpolation was applied before the differential time measurement. The data are interpolated to a sampling interval of 0.3125 ms, which can be considered as the precision of our differential time measurements. The cc is calculated in the time domain using a 1.1 s time window (0.1 s and 1.0 s before and after the onset of the P wave, respectively). To ensure the time window is correctly selected, we manually picked 6089 P wave arrival times for all the available waveform data that have high signal to noise ratio. We selected 83831 pairs with a cc >0.7 for the DD relocation.

3. Results and Discussion

[9] The relocated seismicity reveals a narrow fault zone at most locations along the Tangshan fault (Figure 2). Most of the events occurred within a depth range of ~5–20 km and they define a nearly vertical fault. Geographically, more than 85% of the seismicity is distributed in the northern segment, where the relocated earthquakes form two tight clusters. The northern segment had very small coseismic slips during the 1976 M7.8 Tangshan earthquake, suggest-

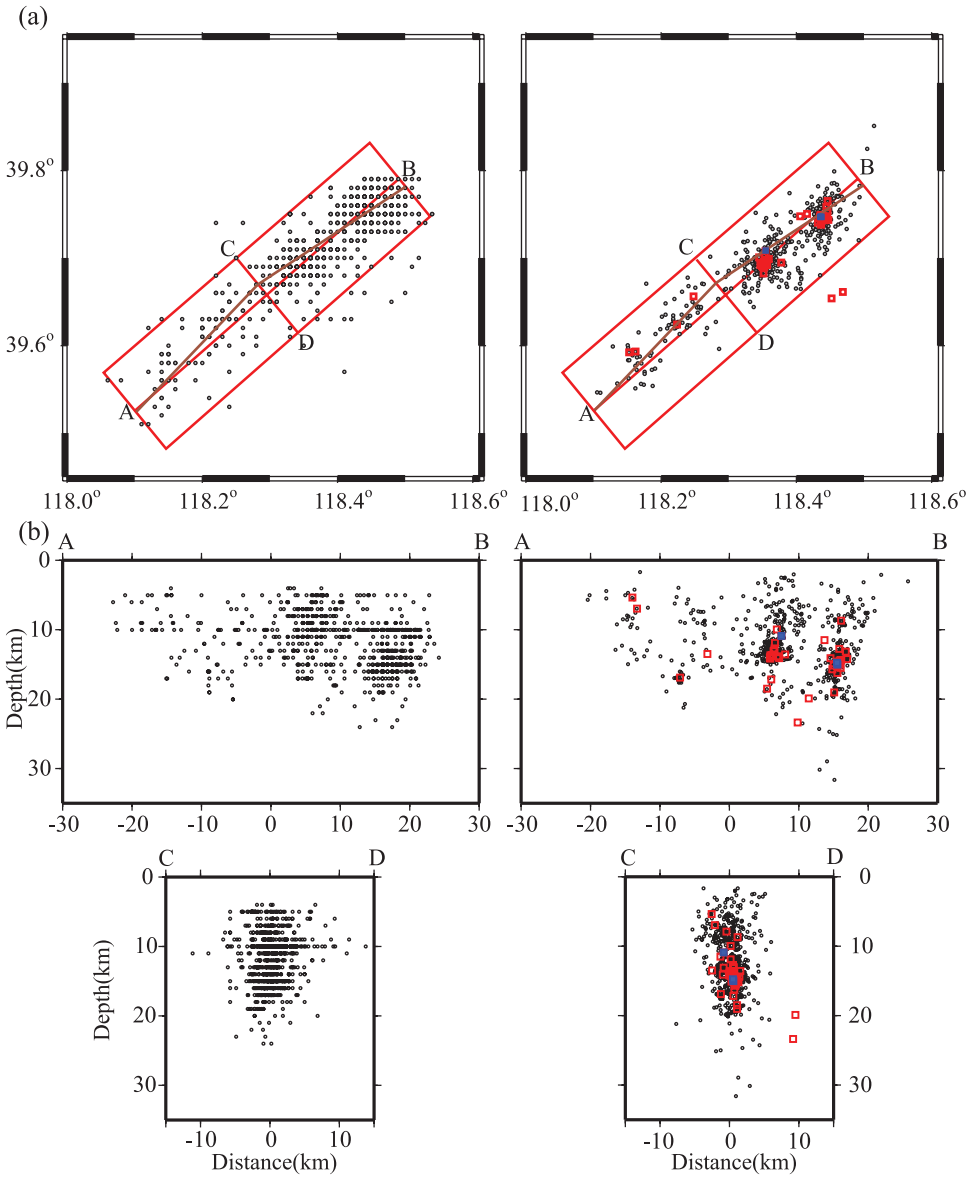

Figure 2. A comparison of (left) BSN catalog locations and (right) DD locations of the seismicity. (a) Map view of seismicity. (b) Depth cross section views of the seismicity. Similar and repeating events are shown by open squares. The three sequences discussed in the text are shown by solid squares. The large lateral scatter in the relocated seismicity reflects either the nature of the seismicity in this intraplate fault or large location errors due to the station coverage.

ing that most of the strain energy in this segment was released with relatively small seismic events. Seismicity in the southern segment is lower and remains diffuse even after relocation. There is also a significant difference in *b* value of the seismicity between the two sections (Figure 3a). The *b* values calculated from the northern and southern section are 1.03 ± 0.02 and 0.85 ± 0.03, respectively. The relative lower seismicity and lower *b* value observed from the southern section can be qualitatively explained by the ENE-WSW oriented compressional stress field resulting from the India-Eurasia collision. Due to this eastward compression, the southern segment experiences a lower shear stress but a higher normal stress compared to the northern segment, resulting a smaller number of earthquakes with relatively larger magnitude that explains the observed lower seismicity and *b* value.

[10] We noticed that many events have similar waveforms during the cc calculation (Figure 3b). If we define similar events to be event clusters having cc $\geq$ 0.8 for a time window 1s before the P wave to 5s after S wave recorded at least one station, we identified a total of 46 similar event sequences with the number of events per sequence ranging from 2 to 130. These comprised 21 doublet and 25 multiplets. The total number of earthquakes in the 46 sequences is 328, making up to 53% of the entire seismicity (619 events). We found significant variations in the recurrence time interval in each sequence, ranging from a few minutes to hundreds of days. Event magnitude in each sequence also varies substantially. 12 doublets and 3 multiplets have recurrence interval less than 10 days. Another 3 doublets and 3 multiplets occurred within a two-month period.

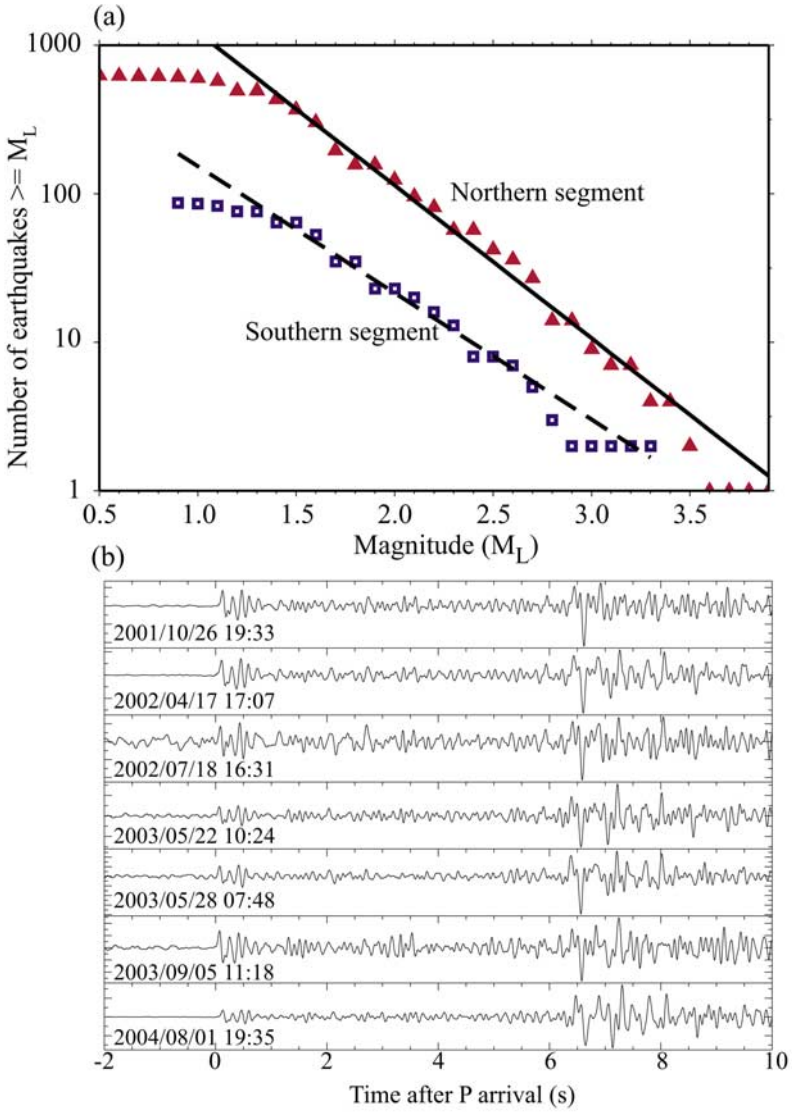

Figure 3. (a) Cumulative frequency-magnitude distributions for the northern (solid triangles) and southern (open squares) segment. An increment of 0.1 in magnitude is used to calculate the cumulative event numbers. (b) Examples of seismograms of sequence 1 recorded at the broadband station QIX station.

[11] Besides the repeating events, some immediate aftershocks have also been observed to exhibit very similar waveforms [e.g., *Cheng et al.*, 2007]. The difference between repeating events and similar aftershocks is defined by their spatial distribution. In principle rupture areas of the repeating events overlap with each other, while those of the similar aftershocks are displaced from one to another. It is likely that the identified sequences include both repeating events and similar aftershocks, resulting in aperiodicity in recurrence interval and large variations in event size in each sequence. Fine relocation of these sequences is thus needed to separate the repeating events from the similar ones.

[12] Most of the BSN stations are located in the northwest side of the fault, resulting in a one-side distribution to the Tangshan earthquakes. Because of the underlying thick sedimentary layer, the BSN stations usually have high noise levels. The one-side station coverage coupled with low signal to noise ratio makes it difficult to determine the accurate locations of the earthquakes. They also affect the task of defining a complete list of events in each sequence, making them appear to be aperiodic.

[13] We applied the following criteria to select multiplets to perform a fine relocation: (1) average cc > 0.85; (2) internal inconsistence in travel time picking <0.5 ms; (3) average recurrence interval >100 days; (4) number of travel time picking >4(N-1), where N is the event number of the multiplet and 4(N-1) is the number of unknowns. Only 3 multiplets satisfied these four requirements. Details of the three sequences are listed in Table S1 of the auxiliary material.[1] For each sequence, we applied the fine relocation method [*Got et al.*, 1994] to the differential travel-time data. We also assume that all the events occurred in the vertical fault plane that derived from a linear regression of the relocated

[1]Auxiliary materials are available in the HTML. doi:10.1029/2007GL031594.

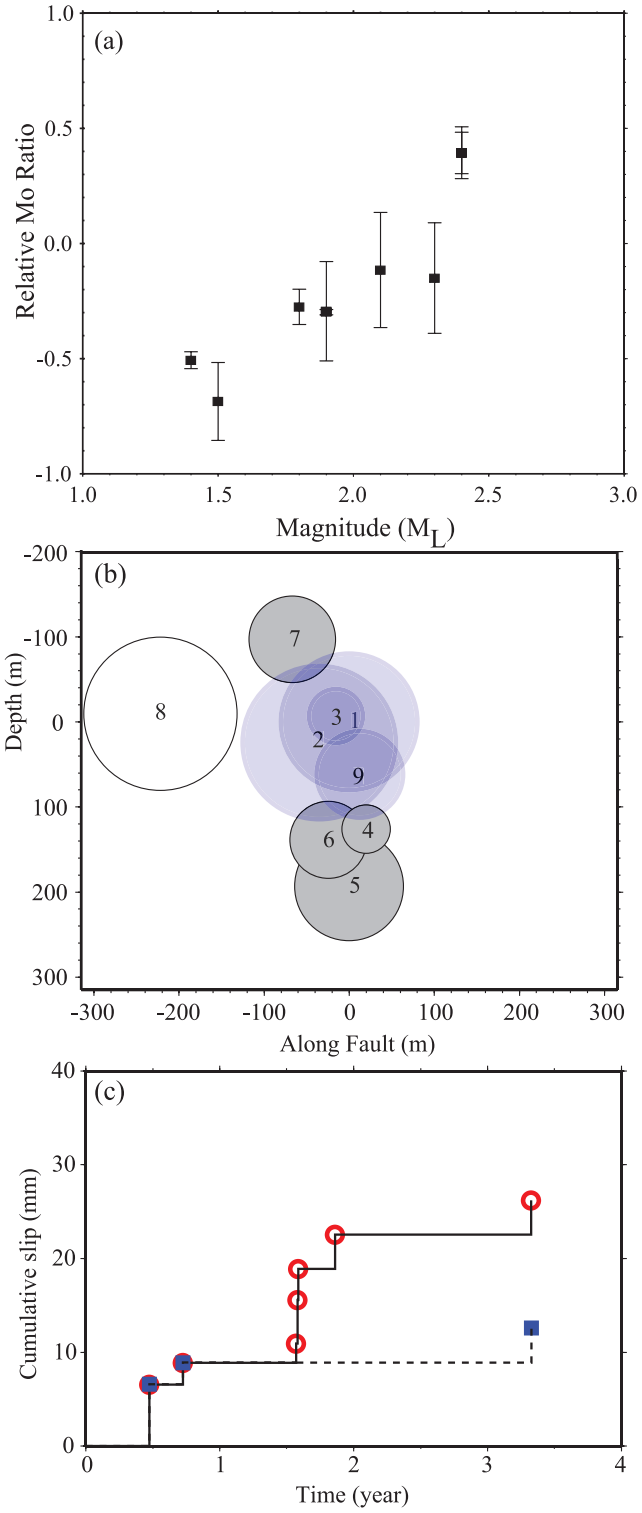

Figure 4. (a) Relative moment ratios calculated from the spectral ratios are shown as a function of local magnitude. Notice the good linear correlation between the two. (b) Depth cross section along the fault plane of the relative locations of the 9 earthquakes in sequence 1. (c) Cumulative slips calculated from a loose cluster consisting of 8 events (except 8 in Figure 4b) and a tight cluster consisting of 4 events (1, 2, 3 and 9) are shown in open circles and solid squares, respectively. Event 1 occured at time zero and is not shown here.

seismicity. The relocation error is in the order of tens meters based on a grid search method assuming a travel time picking uncertainty of 0.5 ms.

[14] To compare distances between similar events with rupture sizes and to calculate fault slip rate, it is necessary to have an objective measurement of earthquake size. Magnitude in the BSN catalog is given in Richter scale. This is done by convolving digital recordings with the instrumental response of the Wood-Anderson seismograph and correcting the local attenuation structure. We first used spectral ratio method [*Vidale et al.*, 1994] to verify how well event magnitude in the catalog was determined. To do this, seismograms of all events in a multiplet were first assembled at a given station. Amplitude spectra were then calculated from a 20s time window that includes both P and S waves. These spectra were further stacked to form a station average, which was used to normalize the individual spectrum. The normalized spectra, the spectral ratios, were computed for every station and event. The spectral ratios were reassembled on event base and were subsequently averaged to form an event spectra ratio. The relative moments are finally measured from the spectral ratio averaged in the frequency range of 1 to 10 Hz. There is an excellent linear correlation between the logarithm of relative moments and M_L (Figure 4a), indicating that relative magnitude in the BSN catalog is well determined (Figure 4a).

[15] We then used the moment-magnitude relationship of *Hanks and Kanamori* [1979],

$$\log(M_0) = 16.1 + 1.5M_L \tag{1}$$

to convert M_L to M_o. We further assume a circular rupture model and estimate rupture radius r, from M_o under a given stress drop ($\Delta\sigma$) by using the equation from *Kanamori and Anderson* [1975]:

$$r = \left(\frac{7M_o}{16\Delta\sigma}\right)^{1/3} \tag{2}$$

[16] The coseismic slip is then calculated from the estimated M_o and r:

$$d = M_o/\mu\pi r^2 \tag{3}$$

[17] Figure 4b shows an example of the distribution of the relocated events in sequence 1. The size of the circle represents the rupture area which was calculated based on equation (2) with a stress drop of 3 MPa. It appears that event 8 lies outside the cluster, and events 4, 5 and 6 are another subgroup. Event 7 also barely overlaps with other events. If we define a loose cluster that includes all the events except for event 8, then we obtained an annual slip rate of 7.1 ± 1.6 mm/yr using a linear regression of the cumulative slip shown as open circles in Figure 4c. As the 8 events did not occur at the same patch, the released strains should not be solely built up within the recurrence intervals. Thus the annual slip rate here should be considered as an over estimate of the actual stress build up along the fault. If we used the four events (1, 2, 3 and 9) that have better overlaps, we obtained an annual slip rate of 2.6 ± 0.4 mm/yr.

[18] The relocated results for the three sequences are summarized in Table S1. For sequence 2, only the first and third events overlap with each other. Using these two events, we obtained an annual slip rate of 7.6 mm/yr. Because of the partial overlap, this value should be also considered as an overestimation. For the 3rd sequence, we have very few observations for three members (marked as x in Table S1), and there are no statistically significant overlaps among the rest events.

[19] GPS measurement showed that the surface of North China basin is overall moving to the east with respect to the stable Eurasia [*Wang et al.*, 2001]. The geodetic data also revealed significant internal deformations, suggesting that part of the eastward motion is likely devoted to the strain buildup along the Tangshan fault. Our estimate of a slip rate of 2.6 mm/yr thus agrees with the surface GPS measurement. *Cheng et al.* [2007] found no repeating earthquakes along an intraplate fault in central Japan, which they attributed to the lack of a weak zone along the fault. The presence of a large amount of similar and repeating events along the Tangshan fault suggests that damage zone of the 1976 earthquake remains weak since the earthquake. The seismicity is unevenly distributed along the fault, surrounded by weak areas that undergo stable creep under steady tectonic loading.

4. Conclusions

[20] We have investigated seismicity along the Tangshan fault in 2001–2006. We found that: (1) the seismicity clearly exhibits a dextral bend in the middle of the fault and more than 85% of the events occurred in the northern segment where relatively small coseismic slips were observed during the 1976 M7.8 earthquake; (2) the two segments have significantly different b values, 1.03 ± 0.02 and 0.85 ± 0.03 for the northern and southern sections, respectively; (3) approximately 53% of the earthquakes are similar or repeating events, exhibiting a highly clustering feature of the seismicity in space; (4) the annual slip rate along the northern section of the fault is no larger than 2.6 ± 0.4 at seismogenic depth, consistent with surface GPS observations. The distinct seismicity and b values are probably the collective effect of the fault geometry and the regional stress field. The high percentage of similar and repeating events suggested that the intraplate Tangshan fault has a well developed weak zone that is characterized by many mature interplate faults.

[21] **Acknowledgments.** We thank the CEA network center for providing data, and two anonymous reviewers for constructive comments. This study was supported by Ministry of Science and Technology of China under grant 2005DFA20980, NSF grant EAR-0352134, and an international travel grant from Rice University.

References

Cheng, X., F. Niu, P. G. Silver, S. Horiuchi, K. Takai, Y. Iio, and H. Ito (2007), Similar microearthquakes observed in western Nagano, Japan, and implications for rupture mechanics, *J. Geophys. Res.*, *112*, B04306, doi:10.1029/2006JB004416.

Got, J.-L., J. Frechet, and F. W. Klein (1994), Deep fault plane geometry inferred from multiplet relative relocation beneath the south flank of Kilauea, *J. Geophys. Res.*, *99*, 15,375–15,386.

Gutenberg, B., and C. F. Richter (1944), Frequency of earthquakes in California, *Bull. Seismol. Soc. Am.*, *34*, 185–188.

Hanks, T. C., and H. Kanamori (1979), A moment magnitude scale, *J. Geophys. Res.*, *84*, 2348–2350.

Igarashi, T., T. Matsuzawa, and A. Hasegawa (2003), Repeating earthquakes and interplate aseismic slip in the northeastern Japan subduction zone, *J. Geophys. Res.*, *108*(B5), 2249, doi:10.1029/2002JB001920.

Kanamori, H., and D. L. Anderson (1975), Theoretical basis for some empirical relations in seismology, *Bull. Seismol. Soc. Am.*, *65*, 1073–1095.

Nabelek, J., W. P. Chen, and H. Ye (1987), The Tangshan earthquake sequence and its implications for the evolution of the North China Basin, *J. Geophys. Res.*, *92*, 12,615–12,628.

Nadeau, R. M., and L. R. Johnson (1998), Seismological studies at Parkfield VI: Moment release rates and estimates of source parameters for small repeating earthquakes, *Bull. Seismol. Soc. Am.*, *88*, 790–814.

Rubin, A. M., D. Gillard, and J.-L. Got (1999), Streaks of microearthquakes along creeping faults, *Nature*, *400*, 635–641.

Schaff, D. P., and P. G. Richards (2004), Repeating seismic events in China, *Science*, *303*, 1176–1178.

Scholz, C. H. (1968), The frequency-magnitude relation of micro fracturing in rock and its relation to earthquakes, *Bull. Seismol. Soc. Am.*, *58*, 399–415.

Schorlemmer, D., and S. Wiemer (2005), Microseismicity data forecast rupture area, *Nature*, *434*, 1086, doi:10.1038/4341086a.

Shedlock, K. M., J. Baranowski, W. Xiao, and X. L. Hu (1987), The Tangshan aftershock sequence, *J. Geophys. Res.*, *92*, 2791–2803.

Vidale, J. E., W. L. Ellsworth, A. Cole, and C. Marone (1994), Variations in rupture process with recurrence interval in a repeated small earthquake, *Nature*, *36*, 8624–8626.

Waldhauser, F., and W. L. Ellsworth (2000), A double-difference earthquake location algorithm: Method and application to the northern Hayward fault, California, *Bull. Seismol. Soc. Am.*, *90*, 1353–1368.

Waldhauser, F., and W. L. Ellsworth (2002), Fault structure and mechanics of the Hayward Fault, California, from double-difference earthquake locations, *J. Geophys. Res.*, *107*(B3), 2054, doi:10.1029/2000JB000084.

Wang, Q., et al. (2001), Present-day crustal deformation in China constrained by Global Positioning System (GPS) measurements, *Science*, *294*, 574–577.

Q.-F. Chen and L. Li, Institute of Earthquake Science, China Earthquake Administration, P.O. Box 166, No. 63 Fuxing Road, Beijing 10036, China. (lile@seis.ac.cn)

X. Cheng and F. Niu, Department of Earth Science, Rice University, 6100 Main Street, Houston, TX 77005, USA.